universität wien

FWF Der Wissenschaftsfonds.

Improved time integration for WENO methods in astrophysical applications

Friedrich Kupka

Faculty of Mathematics

University of Vienna, Austria

Contributors and Collaborators

Inmaculada Higueras

Universidad Pública de Navarra, Pamplona, Spain

Othmar Koch

ASC, Vienna University of Technology, Austria

Natalie Happenhofer

Faculty of Mathematics, University of Vienna, Austria

Hannes Grimm-Strele, Herbert Muthsam

Bernhard Löw-Baselli

Faculty of Mathematics, University of Vienna, Austria

Jérôme Ballot

Laboratoire d'Astrophysique, Obs. de Midi-Pyréenées, Toulouse, France

Motivation I

The problem of time step restrictions

- *given a physical system and a set of dynamical equations dy(t)/dt = f(y(t)) describing its evolution in time*
- compute approximate solution as a function of time: $Y_n = Y_n(t) = Y(t_n) \sim y(t_n)$
- between t_n and t_{n+1} such that the solution $Y(t)$ changes only by a few percent:
  $|Y_{n+1} - Y_n| < C\,|Y_n|$ with $C \sim 0.05 \ldots 0.1$ ➔ sufficiently accurate advancing
- explicit integration methods require to resolve the time dependence of all the processes described by the equations (independent of their amplitude, etc.):
  $|Y_{n+1} - Y_n| < D\,|Y_n|$ with $D \ll C$
- implicit methods can be less restrictive and ideally reach $D \sim C$ with $D \leq C$
- but additional properties are often required for acceptable approximations
- fully implicit methods are expensive... so, how to get around this ?

Motivation II

Motivation for methods discussed below

- for a two-species flow as in the problem of double-diffusive convection the Navier-Stokes equation can be recast as

$$\underbrace{\frac{d}{dt}\begin{pmatrix}\rho\\ \rho c\\ \rho\mathbf{u}\\ e\end{pmatrix}}_{\dot{y}(t)} = \underbrace{-\nabla\cdot\begin{pmatrix}\rho\mathbf{u}\\ \rho c\mathbf{u}\\ \rho\mathbf{u}\otimes\mathbf{u}+P-\sigma\\ e\mathbf{u}+P\mathbf{u}-\mathbf{u}\cdot\sigma\end{pmatrix}-\begin{pmatrix}0\\ 0\\ \rho g\\ \rho g\mathbf{u}\end{pmatrix}}_{F(y(t))} + \underbrace{\nabla\cdot\begin{pmatrix}0\\ \rho\kappa_c\nabla c\\ 0\\ K\nabla T\end{pmatrix}}_{G(y(t))}$$

- perhaps split off pressure terms (→ Kwatra's method, see below) & viscosity, too
- solve this system numerically as follows:
  - Method of lines (MOL): spatial derivatives discretized by, e.g., a finite difference or finite volume approach such as the weighted essentially non-oscillatory (WENO) method. Similar for boundary conditions.
  - Result: a set of non-linear, coupled ordinary differential equations (ODEs).

Motivation III

Astrophysical convection simulations

- typical simulations of M dwarf, idealised semiconvection with Pr=0.1, Cepheid

$c_{ad} = c_{diff} = 0.2$	Δt_{ad}	Δt_{snd}	Δt_{diff}
Convection (M-Star)	7 s	0.52 s	383 s
Semiconvection	19.47 s	2.45 s	3.72 s
Cepheid	2.31 s	1.73 s	0.057 s

- M dwarf: time step limited by sound waves: low Mach number flow
- Semiconvection: low Mach number flow, limited by heat diffusion until the layer becomes convective (transition diffusive ➜ advective during simulation)
- Cepheid: limited by radiative diffusion in layers near / at the surface (also in A-type stars, red giants, AGB stars, ...)

Motivation IV

Why splitting instead of fully implicit ?

- in hydrodynamics: little gain from implicitly integrating the advection operator
  - if it is limiting Δt ➔ solution usually changes on Δt
  - for order in time $p > 1$: strong stability (SSP) property is lost, if $\Delta t > 4\, \Delta t_{adv}$

    ➔ Kraaijevanger: BIT 31, 482 (1991); Ferracina & Spijker: Math. Comp. 74, 201 (2004), Appl. Num. Math. 58, 1675 (2008); Ketcheson et al.: Appl. Num. Math. 59, 373 (2008), J. Sci. Comp. 38, 251 (2009)
- if the NSE are integrated in time with IMEX RK-methods, generalized (linear or quasilinear) Helmholtz equations are obtained (scalar, computationally cheaper)
- the same holds for the method of Kwatra et al. (2009), JCP 228, 4146 used for semi-implicit integration of terms containing ∇p
- these are (quasilinear) elliptic equations (even V-coercive and V-elliptic)
- fast, well-converging methods available: CG-type, multigrid methods

Kwatra's method I

Summary

- following Kwatra et al. (2009), JCP 228, 4146 use Dp/Dt, equation of state, and conservation laws to derive a dynamical equation for ∂p/∂t. Then
  - discretize "diffusion-like" terms at t_{n+1}, evaluate other terms at t_n
  - construct (discretized) equation for p_{n+1}
  - additive pressure-term splitting as in incompressible methods → $(u_{n+1})^*$
  - compressibility → use discretized equation for p_{n+1} to predict $(p_{n+1})^*$
  - use $(p_{n+1})^*$ to complete time step → u_{n+1}, evaluate final p_{n+1} form EOS
  - in RK methods repeat at each stage, in IMEX RK assign p_{n+1} to "explicit part"
- also with buoyancy source term (→ explicit, e.g.) & diffusion terms (→ right-hand side of generalized Helmholtz equations) (Happenhofer et al. 2013, JCP 236, 96)
- can be used in low and high Mach number regime
- time step limit from advection and steep pressure gradients, not sound waves (!)

Kwatra's method II

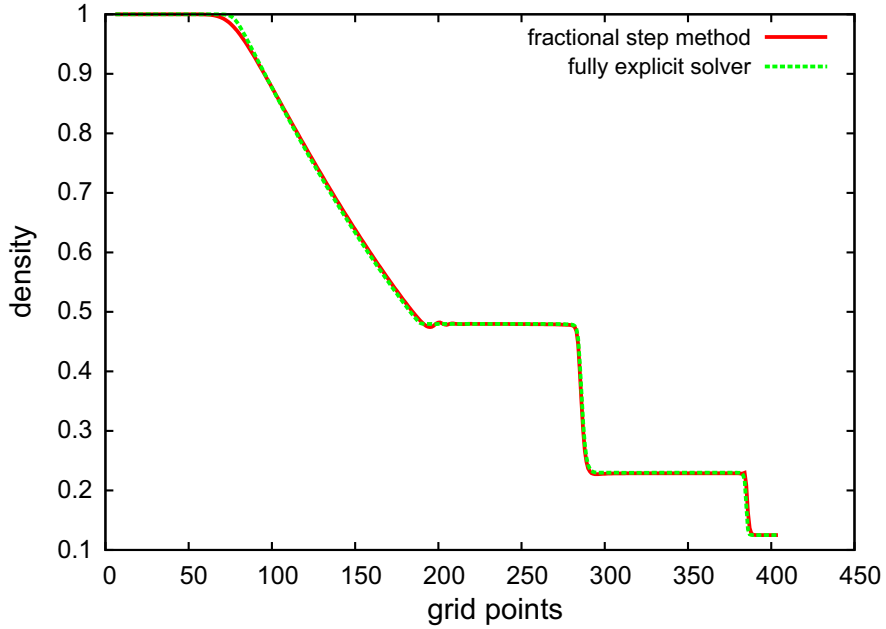

(a) Density

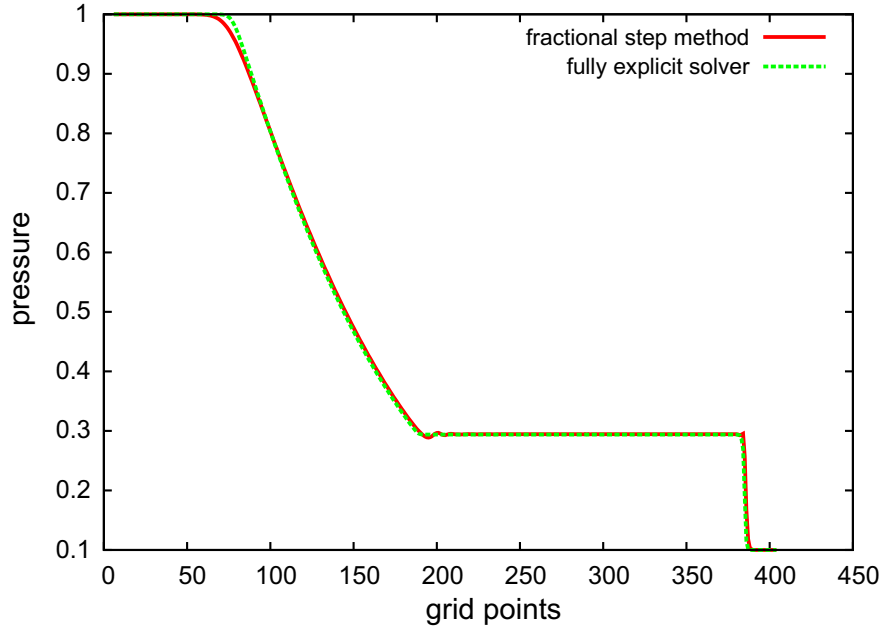

(b) Pressure

Fig. 8. Results of the Sod shocktube test at $t = 0.25$ s. Density and Pressure are plotted against an explicit reference solution. The results indicate well resolved shock waves.

1D Sod shocktube test with 405 grid points taken from Happenhofer et al. (2013), JCP 236, 96 confirming Kwatra et al. (2009), JCP 228, 4146

Kwatra's method III

Table 8
Timing results from the smooth flow test for different Courant numbers. Simulation time is $t = 2.5 \times 10^{-5}$ s.

Method	CFL-number	Timestep Δt	Wallclocktime
Explicit	0.5	1.53×10^{-8}	01:18:04
Semi-implicit	0.5	1.53×10^{-8}	00:35:04
Semi-implicit	3	9.18×10^{-8}	00:06:33
Semi-implicit	30	9.18×10^{-7}	00:01:59
Semi-implicit	300	9.18×10^{-6}	00:00:20

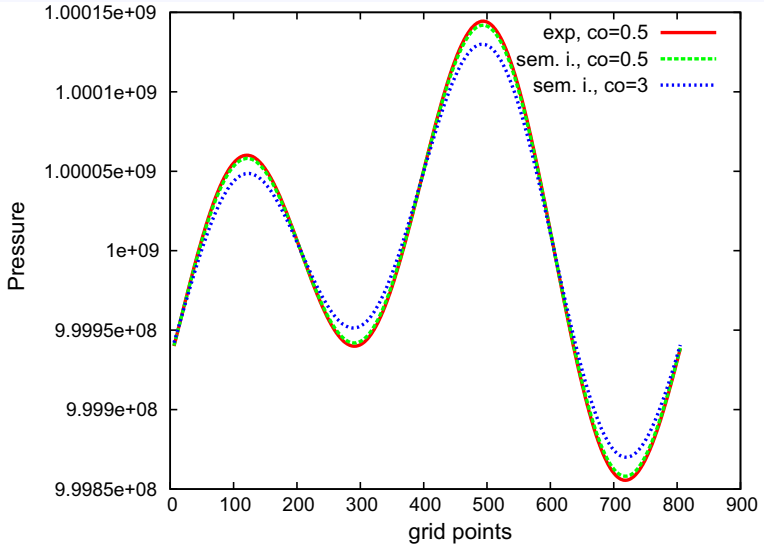

Fig. 10. Numerical results comparing the pressure at $t = 1.25 \times 10^{-5}$ s in the smooth flow test run with different CFL numbers.

1D smooth, low Mach number flow test test from Happenhofer et al. (2013), JCP 236, 96 confirming Kwatra et al. (2009), JCP 228, 4146

Kwatra's method IV

Table 5
Fractional step method scaling test (1600×1600 grid points), calculated at the Vienna Scientific Cluster 2 (VSC2).

# Cores	Time in s
1	Estimate: 7.3 days
16	23:52:50
64	05:53:13
256	01:20:02
1024	00:26:32

Table 6
Fractional step method scaling test (3200×3200 grid points), calculated at the Vienna Scientific Cluster 2 (VSC2).

# Cores	Time in s
256	24:15:00
1024	06:39:44
2048	04:44:25
4096	04:38:15

Table 7
Explicit solver scaling test (3200×3200 grid points), calculated at the Vienna Scientific Cluster 2 (VSC2).

# Cores	Time in s
1024	02:11:21
2048	01:42:29
4096	01:22:03

scaling test of simulation of fully compressible convection ($Ra=1.6 \times 10^6$, $Pr = 0.1$, run over 0.5 sound crossing times), from Happenhofer et al. (2013), JCP 236, 96

further tests passed: convergence rate, 2D circular shock (from Kwatra et al.), 2D Gresho vortex test (new test, for Ma = 0.1 to 0.001)

Improved Time Integration

IMEX RK-Methods I

Definition of IMEX RK-Methods

Consider the ODE initial value problem

$$\dot{y}(t) = F(y(t)) + G(y(t)), \qquad y(0) = y_0, \tag{1}$$

where the vector fields F and G have different stiffness properties.

An s-stage Runge–Kutta method characterized by coefficient matrices $A = (a_{i,j})$ and $\tilde{A} = (\tilde{a}_{i,j})$ defines one step $y_{\text{old}} \to y_{\text{new}}$ by

$$y_i = y_{\text{old}} + \Delta t \sum_{j=1}^{s} a_{i,j} F(y_j) + \Delta t \sum_{j=1}^{s} \tilde{a}_{i,j} G(y_j), \quad i = 1, \ldots, s, \tag{2}$$

$$y_{\text{new}} = y_{\text{old}} + \Delta t \sum_{j=1}^{s} b_j F(y_j) + \Delta t \sum_{j=1}^{s} \tilde{b}_j G(y_j). \tag{3}$$

If $a_{i,j} = 0$ for $j \geq i$, the method is called an *implicit–explicit (IMEX)* method.

(following Kupka et al. (2012), JCP 231, 3561)

IMEX RK-Methods II

Strong Stability Preserving (SSP) property:

- monotonicity: $|u(t)| \leq |u(t_0)|$ $\forall\ t \geq t_0$ with $|.|$ some (semi-)norm
- contractivity: $|u(t)-v(t)| \leq |u(t_0)-v(t_0)|$ $\forall\ t \geq t_0$
- boundedness: $m \leq u(t) \leq M$, if $m \leq u(t_0) \leq M$ $\forall\ t \geq t_0$
  (special cases: m = 0 ➜ positivity, likewise: $|u(t)| \leq M$ $\forall\ t \geq t_0$)
- monotonicity u(t) with respect to v(t): $u(t) \leq v(t)$, if $u(t_0) \leq v(t_0)$ $\forall\ t \geq t_0$

Preserve these using SSP schemes for ODEs:

- if the exact solution is monotonic ➜ also require the same from RK scheme !
- numerical monotonicity: strong stability means $|U_{ni}| \leq |u_n|$ for any stage i and internal stage solution U_{ni} computed at time t_n and also $|u_{n+1}| \leq |u_n|$
  ➜ radius of absolute monotonicity (Kraaijevanger 1991) ➜ restricts step size
- reformulate RK schemes (Shu & Osher 1988) ➜ if for a spatial discretization the Euler forward scheme is strongly stable, then an RK scheme is strongly stable, too (for any scheme: usually only under step size restrictions)

IMEX RK-Methods III

Higueras (2006) develops a comprehensive theory of strong stability preserving additive Runge–Kutta schemes which extends the concepts for standard Runge–Kutta methods in a natural way:

Let $\tau,\ \tilde{\tau}$ be the step-size restrictions for monotonicity of the explicit Euler method for the vector fields F and G, respectively. We define the *region of absolute monotonicity*

$$\mathcal{R}(A,\tilde{A}) = \{(r,\tilde{r}) \in \mathbb{R}^2 : (A,\tilde{A}) \text{ is absolutely monotonous on } [-r,0]\times[-\tilde{r},0]\},$$

where the absolute monotonicity at a point $(r_0,\tilde{r}_0)$ is characterized by algebraic relations for the matrices $A,\ \tilde{A}$. The boundary in the first quadrant, $\partial\mathcal{R}(A,\tilde{A}) \cap \{(r,\tilde{r}) : r,\tilde{r} \geq 0\}$, is denoted as the *curve of absolute monotonicity*. The significance of the region $\mathcal{R}(A,\tilde{A})$ is expressed in the following theorem.

Theorem 1.1 *Let $(A,\tilde{A})$ be absolutely monotonous at $(-r,-\tilde{r})$ with step-size coefficients $\tau,\ \tilde{\tau}$. Then for $h \leq \min\{r\tau,\tilde{r}\tilde{\tau}\}$, diminishing of the norm holds,*

$$\|y_i\| \leq \|y_{\text{old}}\|, \quad i=1,\ldots,s, \qquad \|y_{\text{new}}\| \leq \|y_{\text{old}}\|.$$

(from Kupka et al. (2012), JCP 231, 3561)

IMEX RK-Methods IV

Pareschi & Russo (2005) give an IMEX SSP2(2,2,2) method with nontrivial region of absolute monotonicity ($\gamma = 1 - \frac{1}{\sqrt{2}}$):

$$\begin{array}{c|cc} 0 & 0 & 0 \\ 1 & 1 & 0 \\ \hline A & \frac{1}{2} & \frac{1}{2} \end{array} \qquad \begin{array}{c|cc} \gamma & \gamma & 0 \\ 1-\gamma & 1-2\gamma & \gamma \\ \hline \tilde{A} & \frac{1}{2} & \frac{1}{2} \end{array} . \tag{6}$$

The coefficients imply $\mathcal{R}(A) = 1$, $\mathcal{R}(\tilde{A}) = 1 + \sqrt{2}$, and

$$\mathcal{R}(A, \tilde{A}) = \{(r, \tilde{r}) : 0 \le r \le 1,\ 0 \le \tilde{r} \le \sqrt{2}(1 - r)\},$$

see Higueras (2006).

(from Kupka et al. (2012), JCP 231, 3561)

IMEX RK-Methods V

Higueras (2006) gives an IMEX SSP2(3,3,2) method with nontrivial region of absolute monotonicity:

$$\begin{array}{c|ccc} 0 & 0 & 0 & 0 \\ \frac{1}{2} & \frac{1}{2} & 0 & 0 \\ 1 & \frac{1}{2} & \frac{1}{2} & 0 \\ \hline A & \frac{1}{3} & \frac{1}{3} & \frac{1}{3} \end{array} \qquad \begin{array}{c|ccc} \frac{1}{5} & \frac{1}{5} & 0 & 0 \\ \frac{3}{10} & \frac{1}{10} & \frac{1}{5} & 0 \\ 1 & \frac{1}{3} & \frac{1}{3} & \frac{1}{3} \\ \hline \tilde{A} & \frac{1}{3} & \frac{1}{3} & \frac{1}{3} \end{array} \tag{8}$$

This is a modification of a scheme from Pareschi & Russo (2005), where the latter turned out to have a trivial region of absolute monotonicity. It holds that $\mathcal{R}(A) = 2$ and $R(\tilde{A}) = \frac{5}{9}(\sqrt{70} - 4)$, and

$$\mathcal{R}(A, \tilde{A}) = \{(r, \tilde{r}) : 0 \leq r \leq 1,\ 0 \leq \tilde{r} \leq \phi(r)\},$$

where

$$\phi(r) = \left\{ \frac{1}{4}(-28 + 9r) + \frac{1}{4}\sqrt{1264 - 984r + 201r^2} \right\}.$$

We note that the latter is a correction with respect to Higueras (2006), since we have found r to be necessarily bound by 1 in $\mathcal{R}(A, \tilde{A})$.

(from Kupka et al. (2012), JCP 231, 3561)

Applications I

Simulations of Double-Diffusive Convection

- simulation of semiconvection (based on two-species NSE)
  - 400 × 400 points, Cartesian grid, horizontally periodic, DNS
  - compressible, Kwatra's method to deal with ∇p terms
  - time-steps: 24,000 to 300,000; ~ 6 hours @ 64 MPI-processes; 3 GB per run
- using the ANTARES code (Muthsam et al. (2010), New Astronomy 15, 460)
  - default method: conservative 5th order WENO (also with Marquina flux splitting)
  - parabolic terms consistent with WENO (Happenhofer et al. (2013), JCP 236, 96)
  - 1D, 2D, 3D and various grids (Cartesian, co-moving polar, curvi-linear in prep.)
  - optional: grid refinement, DNS/iLES/LES, radiative transfer, MHD mode
  - various open and closed boundary conditions, one- and two-component fluids
  - flexible microphysics modules, compressible or Boussinesq approximation
  - hybrid parallelization (MPI, optionally OpenMP), modular Fortran95, parallel I/O

Applications II

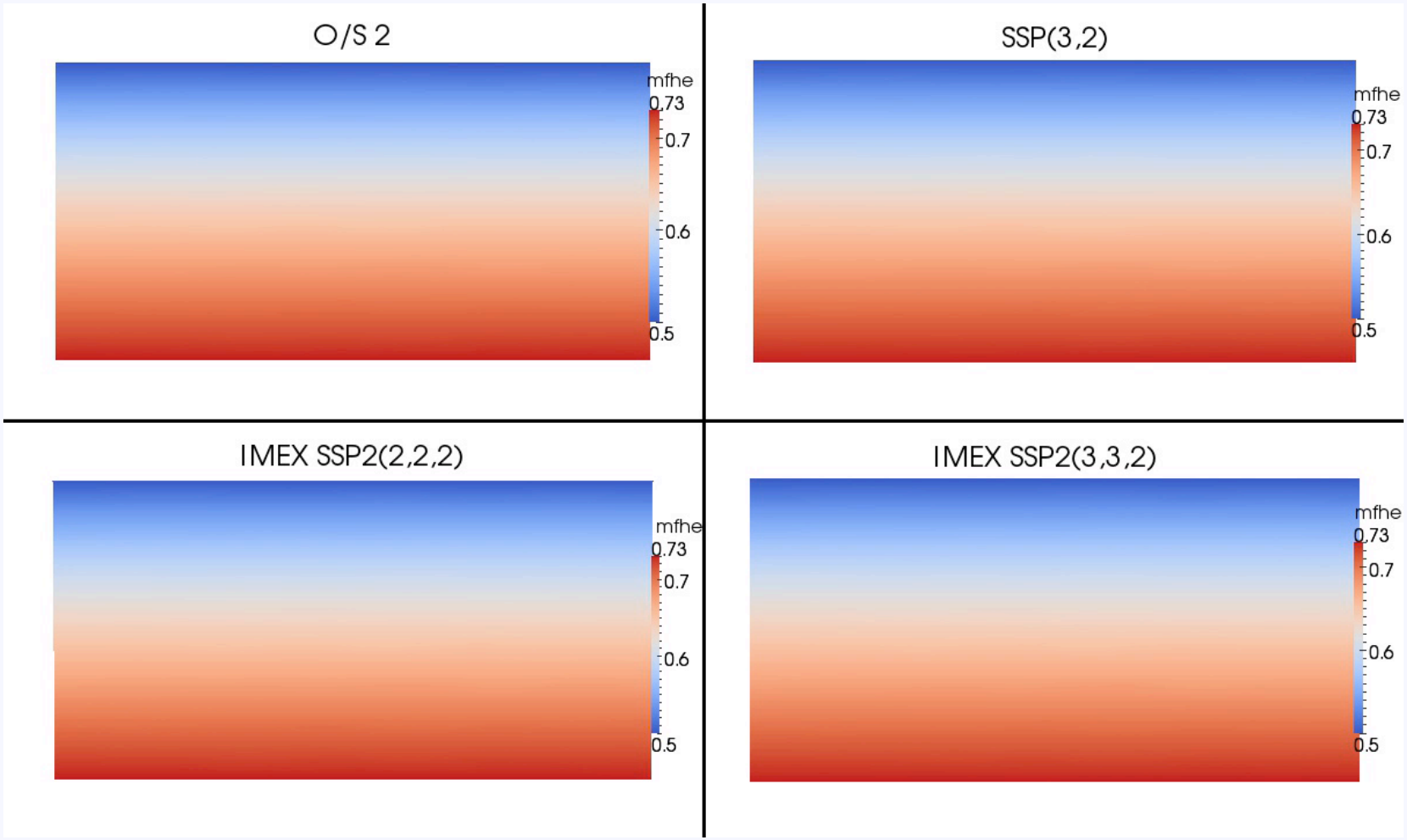

Semiconvection in a compressible layer: explicit vs. semi-implicit time integration.
Computations: N. Happenhofer @ VSC1 (from Kupka et al. 2012, JCP 231, 3561).

Applications III

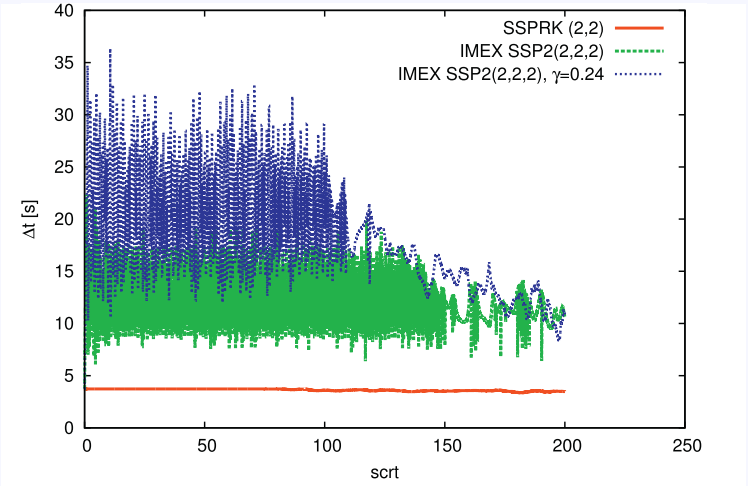

(a) $\mathrm{CFL}_{\mathrm{start}} = 0.2$

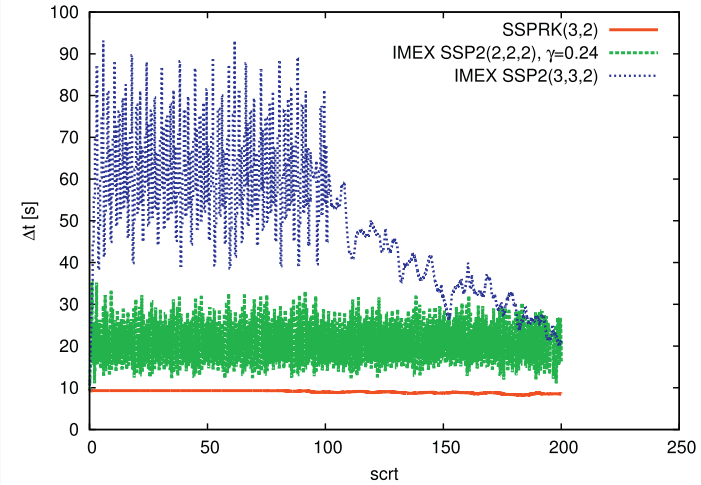

(b) $\mathrm{CFL}_{\mathrm{start}} = 0.5$

Time step size as a function of scrt for the case Pr = 0.1

from Kupka et al. 2012, JCP 231, 3561

Applications IV

Simulations of pulsating Cepheids

- preparing 2D and 3D simulations first consider 1D case: convection-pulsation interacton neglected
- for details on 2D models with explicit time integration see Mundprecht et al. (2013) (submitted to MNRAS, for a preprint see arXiv:1209.2952)
- Cepheid model parameters:
  - T_{eff} = 5125 K, log(g) ~ 1.97, M = 5 $M_\odot$, R ~ 38.5 $R_\odot$, L ~ 913 $L_\odot$, X = 0.7, Y = 0.29, Z = 0.01, P = 3.85 d, first overtone (1O)
  - outer 42% of R, vertical grid spacing: 0.47 Mm ... 124 Mm (modelling only the outer 42% ➜ implies P somewhat too short)
- 1D models: are used to create initial state for the 2D simulations
  - also assume spherical geometry
  - radially stretched grid co-moving with mean pulsation velocity
  - closed boundary conditions

Applications V

Simulation Details: 454 grid points, q=1.007
Dirichlet boundary conditions
Temperature range: 34000 K - 320 000 K

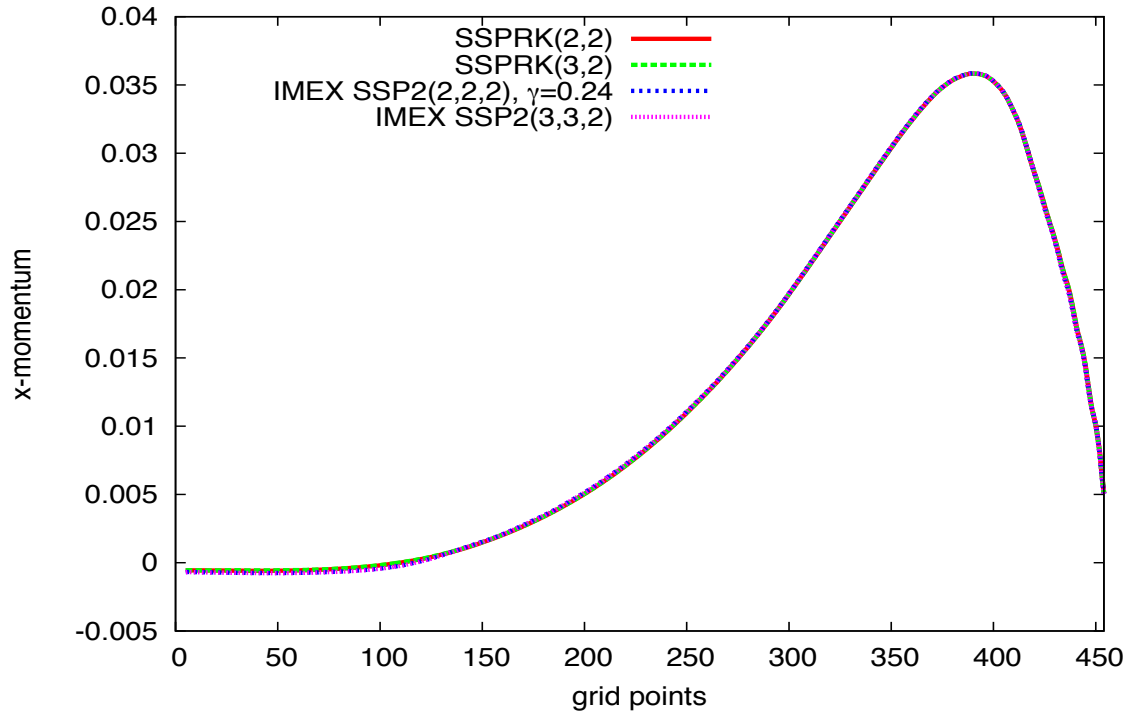

Figure: Comparison of x-Momentum at T=1 scrt.

(courtesy of N. Happenhofer)

Applications VI

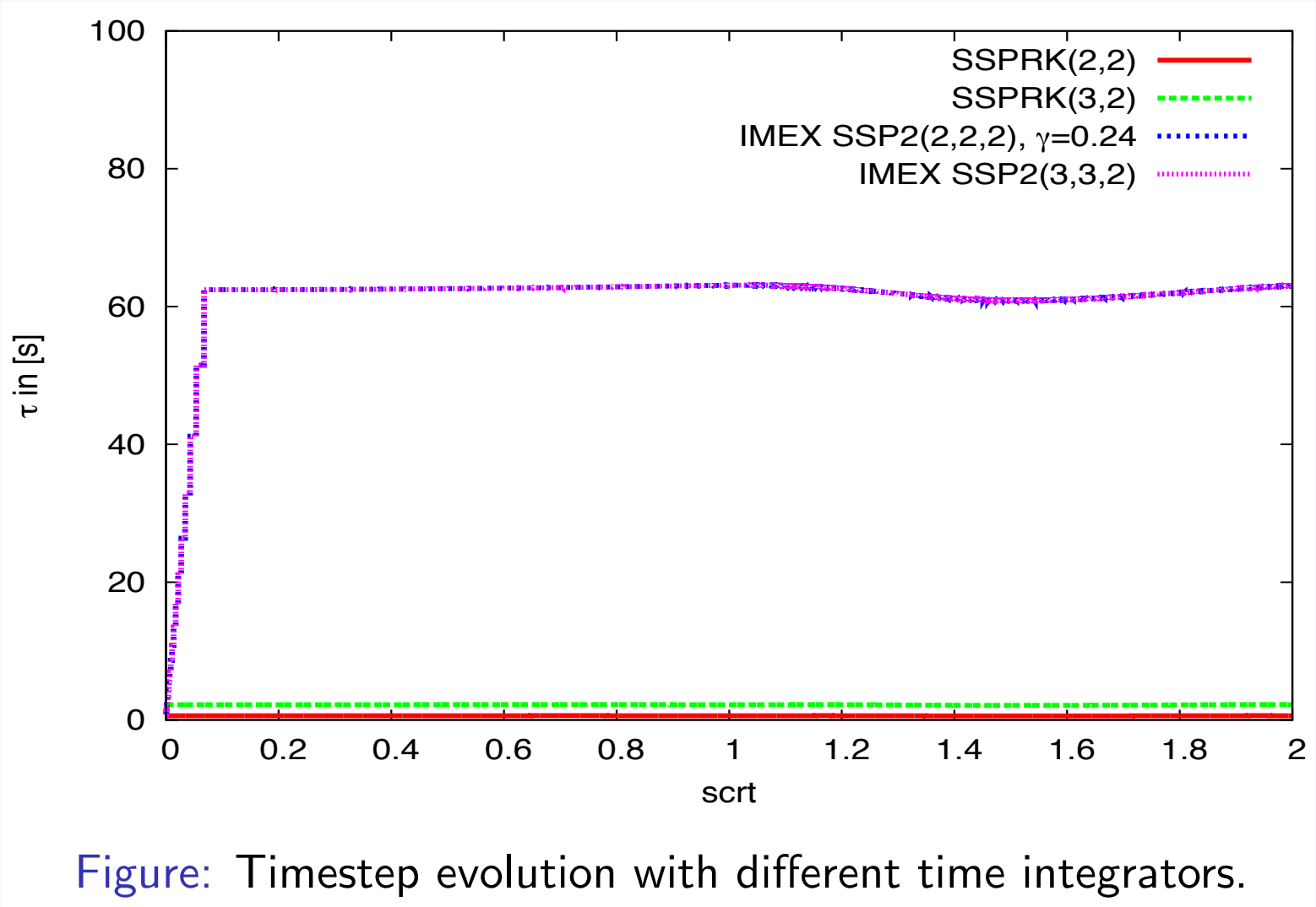

Figure: Timestep evolution with different time integrators.

(courtesy of N. Happenhofer)

Applications VII

1D Deep Cepheid Model				
	Δt_{mean}	$\frac{\Delta t}{\Delta t_{SSPRK(2,2)}}$	$\frac{\Delta t}{\Delta t_{SSPRK(3,2)}}$	WCT
SSPRK(2,2)	0.62 s	1	0.28	6:17:35
SSPRK(3,2)	2.21 s	3.56	1	02:29:31
IMEX SSP2(2,2,2) $\gamma = 0.24$	63.1 s	101.8	18.6	00:13:10
IMEX SSP2(3,3,2)	63.1 s	101.8	18.6	00:16:18

Table: Numerical Results

new IMEX-EWMS methods perform as IMEX SSP2(3,3,2)

(courtesy of N. Happenhofer)

Applications VIII

Is the SSP property really needed for such flows?

- case of semiconvection simulations (400 × 400 points)
  - Kennedy & Carpenter (2003), Appl. Num. Math. 44, 139: ARK3(2)4L[2]SA method
    - fails at CFL_{start} used for IMEX-RK SSP schemes (after 78 time steps)
    - even after 10 scrt never permits to exceed CFL values of explicit schemes !
    - explicitly designed for such systems (L-stable, stiffly accurate, but non-SSP)
  - original Pareschi & Russo, J. Sci. Comp. 25, 129 (2005)) SSP2(3,3,2) scheme
    - at orginal resolution works (SSP in an asymptotic sense: stiffness ➜ infinity)
    - at 100 x 100 points resolution: works during the diffusive phase, fails during the advective phase ($\Delta t \rightarrow 0$ at 113 scrt) (no problem for true SSP schemes)
- case of solar surface convection (2D model with 219 × 159 points)
  - the explicit, non-SSP 3rd order RK method by Heun: found to fail after 9.2 scrt while the SSPRK(3,3) method by Fehlberg (1970) (= TVD3) works for ⩾ 20 scrt
- Cylindrical MHD explosion test (poster by Aloy et al. at this conference):
  - only modified SSP2(3,3,2) scheme works with MCL limiter in the test
  - 3 to 4 time larger time step than original scheme in shock-tube test

New SSP IMEX RK-Methods I

Motivations for further improvements

- Degrees of freedom of RK scheme can be used to fulfil many properties simultaneously instead of just maximizing the region of absolute monotonicity !
- Suggested (Higueras et al. 2013 to be submitted, see ASC Report 14/2012):

1. Overall scheme: second order in time. The error constant should be small. (p=2 O.K., if accuracy is limited by spatial resolution ➜ third order in time not that important).
2. IMEX scheme should be SSP and have a large region of absolute monotonicty (Higueras 2006, 2009) ➜ both the explicit and the implicit schemes must be SSP. The Kraaijevanger radius of each of them should be large, too.
3. The stability function of the implicit scheme should tend to zero at infinitiy, its stability region containing a large subinterval of the negative real axis. Ensured by L-stability.
4. For both schemes, the stability function g should be nonnegative for a large interval of the negative real axis (related to step-size restrictions due to the dissipativity of the spatial discretization). Prevents spurious oscillations of the numerical solution.

Properties 3 & 4 are guided by exact solutions of the heat equation !

New SSP IMEX RK-Methods II

- Further design goals of optimization:
  5. Ensure uniform convergence (to guarantee higher than first order convergence for arbitrarily stiff terms, see Boscarino (2008), SIAM J. Num. Analysis 45, 1600).
  6. For the explicit scheme, the stability region should a) contain large subintervals of the negative real axis, [-z, 0] with $z > 0$, and b) also of the imaginary axis, [-w i, w i] with $w > 0$. The latter requirement is associated with a stable integration of the hyperbolic advection terms (see Motamed et al. 2009, Wang & Spiteri (2007)).
  7. The region of absolute stability of the combined IMEX scheme should be large.
  8. For a convenient and memory-efficient implementation, the coefficients of the scheme should be rational numbers which (recombine the stages in a suitable way).
- Optimize only of the coefficients of the implicit scheme ?
  9. Use optimal second order three stage method by Kraaijevanger (1991), the SSPRK(3,2) method, as explicit method and abandon requirement 6b) from above.
- Possibly consider additional optimizations, if sufficient degrees of freedom are still available ...

New SSP IMEX RK-Methods III

We give the coefficients of the IMEX scheme obtained from our earlier considerations, that is

$$
\begin{array}{c|ccc}
0 & 0 & 0 & 0 \\
\frac{5}{6} & \frac{5}{6} & 0 & 0 \\
\frac{11}{12} & \frac{11}{24} & \frac{11}{24} & 0 \\
\hline
\mathcal{A} & \frac{24}{55} & \frac{1}{5} & \frac{4}{11}
\end{array}
\qquad
\begin{array}{c|ccc}
\frac{2}{11} & \frac{2}{11} & 0 & 0 \\
\frac{289}{462} & \frac{205}{462} & \frac{2}{11} & 0 \\
\frac{751}{924} & \frac{2033}{4620} & \frac{21}{110} & \frac{2}{11} \\
\hline
\tilde{\mathcal{A}} & \frac{24}{55} & \frac{1}{5} & \frac{4}{11}
\end{array}
\tag{22}
$$

and summarize its properties.

This is a second order IMEX scheme such that the implicit method is L–stable. The stability functions for the explicit and implicit schemes are

$$
R_{\mathbb{A}}(z) = 1 + z + \frac{z^2}{2} + \frac{5}{36}\, z^3\,, \qquad R_{\tilde{\mathbb{A}}}(z) = \frac{11\left(13\, z^2 + 110\, z + 242\right)}{2\,(11 - 2\, z)^3}\,. \tag{23}
$$

(see ASC Report 14/2012 and Higueras et al. (2013) to be submitted)

New SSP IMEX RK-Methods IV

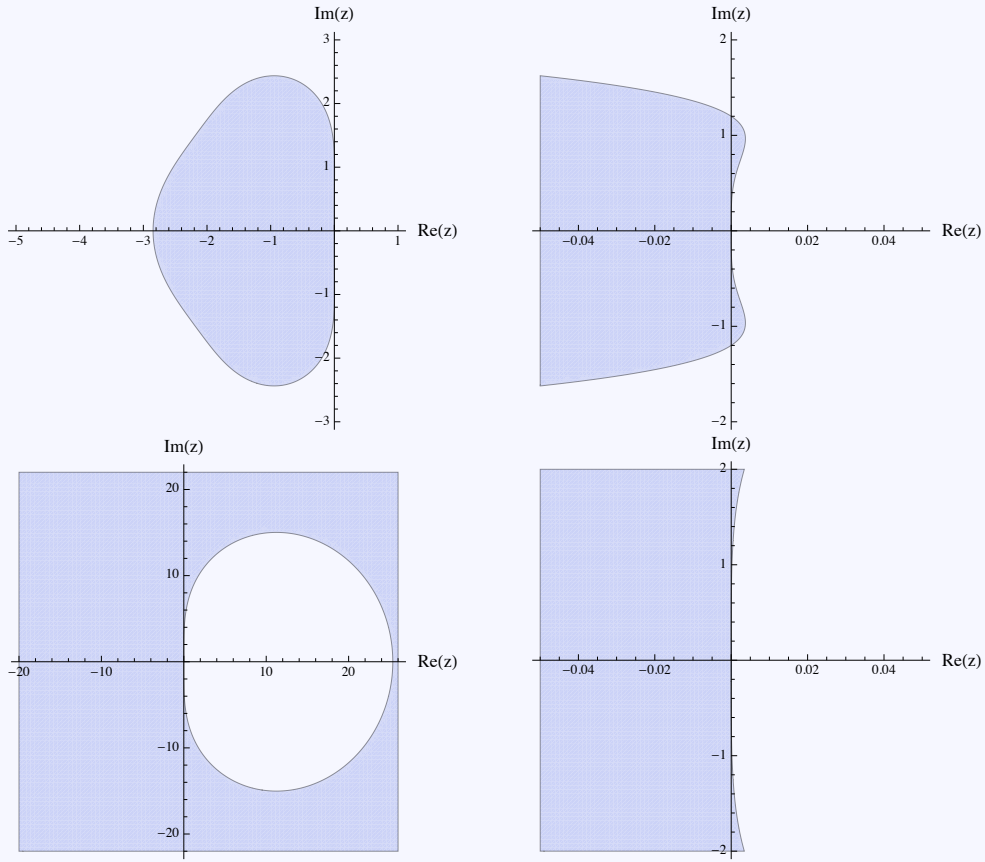

FIG. 3.5. *Stability region and a zoom of the stability region of the explicit scheme in* (3.30) *(top) and the implicit scheme in* (3.30) *(bottom).*

(see ASC Report 14/2012 and Higueras et al. (2013) to be submitted)

New SSP IMEX RK-Methods V

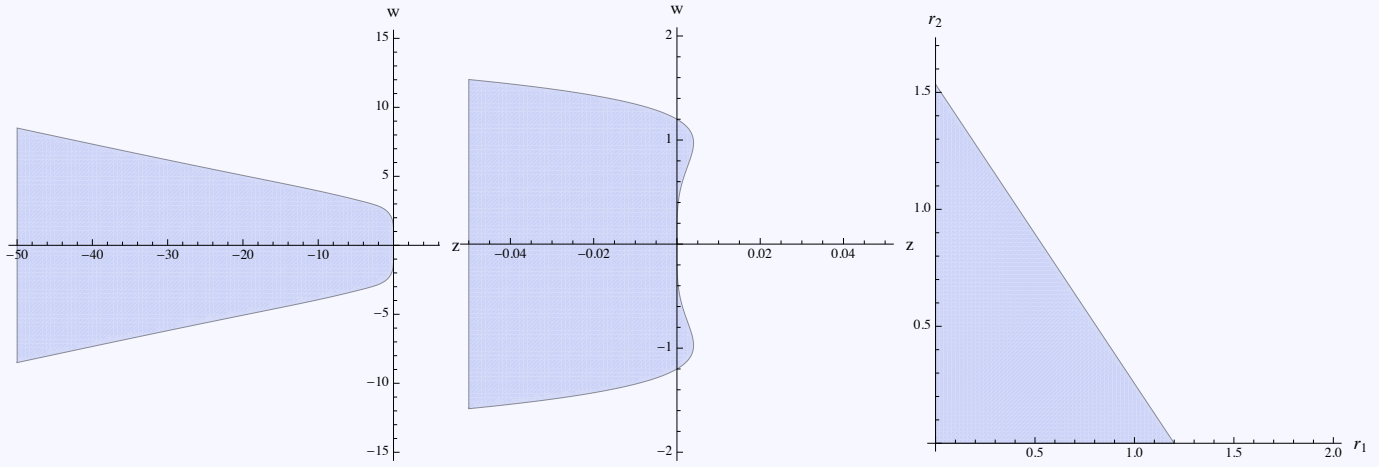

FIG. 3.6. *For IMEX* (3.30)*: stability region (right), a zoom of the region at the origin (center) and region of absolute monotonicity (right).*

Due to the properties listed above, we will refer to to this scheme as SSP2(3,3,2)–LSPUM, where the letters have the following meanings:

'L': L–stable;
'S': the stability region for the explicit part contains an interval on the imaginary axis;
'P': the amplification factor g is always positive;
'U': the IMEX method features uniform convergence (21);
'M': the IMEX method has a nontrivial region of absolute monotonicity.

(see ASC Report 14/2012 and Higueras et al. (2013) to be submitted) (24)

New SSP IMEX RK-Methods VI

IMEX method based on the explicit SSP(3,2) scheme with uniform convergence: in this case, the IMEX scheme obtained by imposing (21) is given by the coefficient tableaux

$$\begin{array}{c|ccc} 0 & 0 & 0 & 0 \\ \frac{1}{2} & \frac{1}{2} & 0 & 0 \\ 1 & \frac{1}{2} & \frac{1}{2} & 0 \\ \hline \mathcal{A} & \frac{1}{3} & \frac{1}{3} & \frac{1}{3} \end{array} \qquad \begin{array}{c|ccc} \frac{2}{11} & \frac{2}{11} & 0 & 0 \\ \frac{69}{154} & \frac{41}{154} & \frac{2}{11} & 0 \\ \frac{67}{77} & \frac{289}{847} & \frac{42}{121} & \frac{2}{11} \\ \hline \tilde{\mathcal{A}} & \frac{1}{3} & \frac{1}{3} & \frac{1}{3} \end{array} \tag{25}$$

Due to its properties, we refer to method as SSP2(3,3,2)–LPUM.

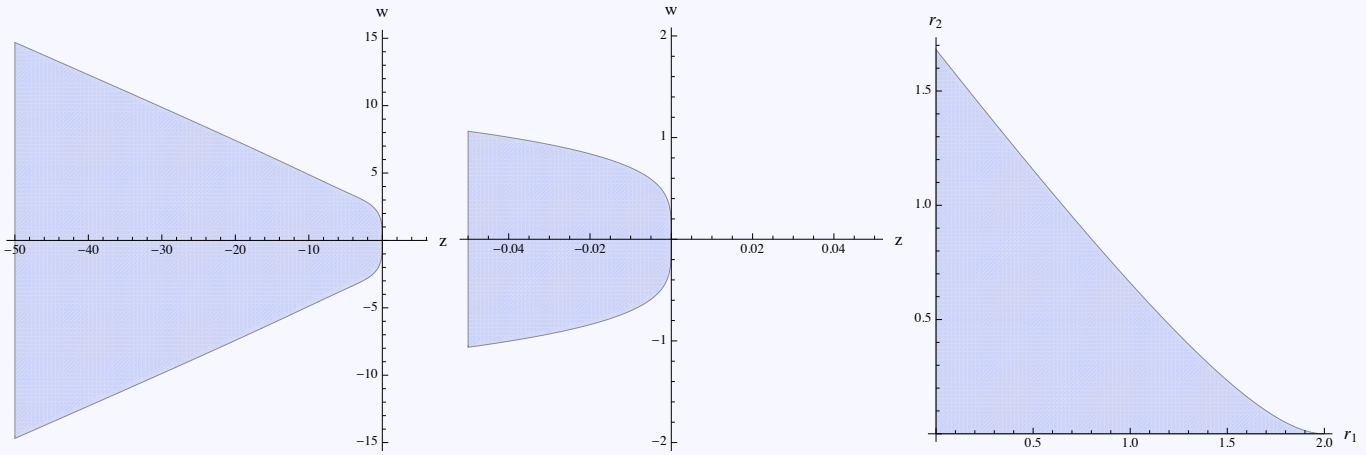

FIG. 4.1. *For the IMEX method* (4.2)*: Left: Stability region; center: zoom of the stability region; right: region of absolute monotonicity.*

(see ASC Report 14/2012 and Higueras et al. (2013) to be submitted)

Results I

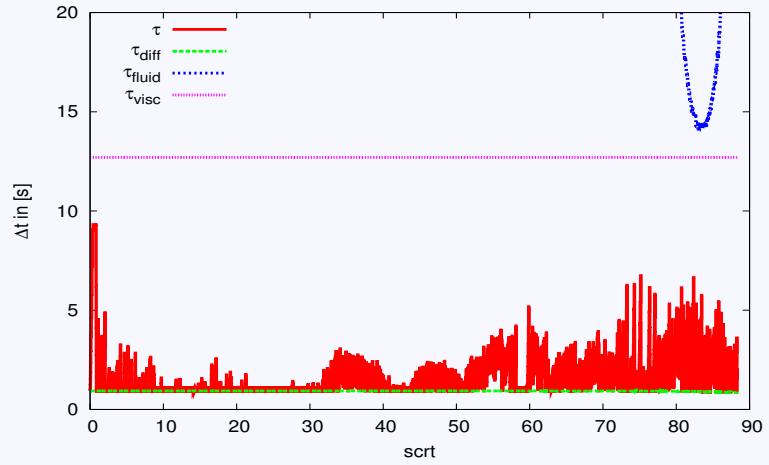

FIG. 5.1. *Simulation A: Time–step evolution with time integrator IMEX SSP1(1,1,1)–LPM.*

case with Pr = 0.1

failure of Euler forward-backward scheme, i.e. IMEX SSP1(1,1,1)-LPM.

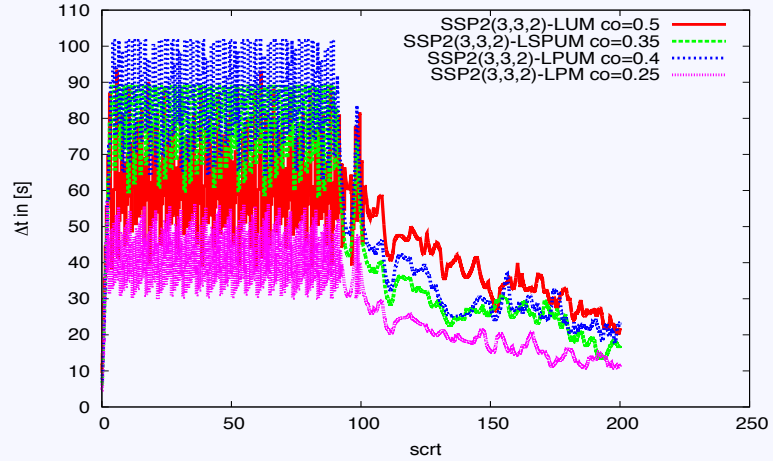

FIG. 5.2. *Simulation A: Time–step evolution over the entire 200 scrt.*

case with Pr = 0.1

LUM-scheme is previously best method: modified SSP2(3,3,2)

(see ASC Report 14/2012 and Higueras et al. (2013) to be submitted)

Results II

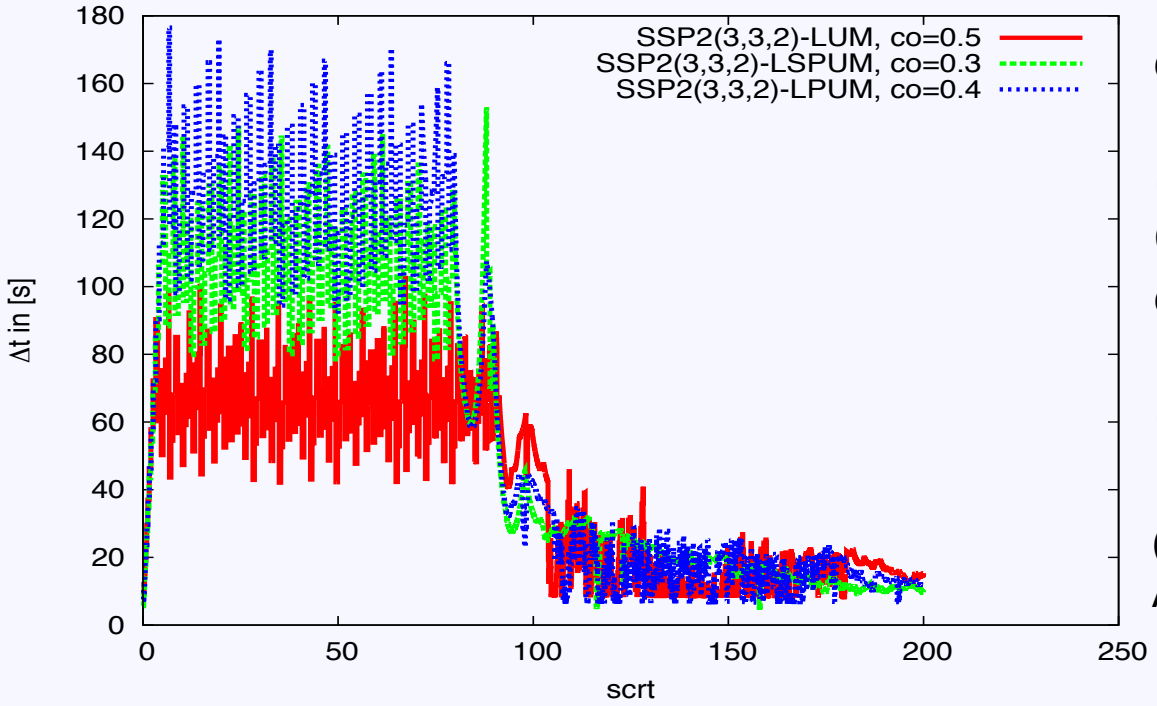

case with Pr = 0.05

(based on pre-cond. CG solver and Schur complement, see Happenhofer et al. (2013), JCP 236, 96)

(data from Higueras et al., ASC Report 14/2012)

FIG. 5.3. *Simulation B: Time–step evolution over the entire 200 scrt.*

SSP2(3,3,2)–LSPUM (3.30)		
Resolution	CFL_{mn}	CFL_{max}
200x200	1.27	4.55
400x400	4.90	7.88
800x800	5.00	8.56
1600x1600	5.09	8.23

SSP2(3,3,2)–LPUM (4.2)		
Resolution	CFL_{mn}	CFL_{max}
200x200	1.27	4.55
400x400	5.73	9.48
800x800	5.71	10.27
1600x1600	6.47	10.19

TABLE 5.3

Resolution Test for Simulation B. Left: SSP2(3,3,2)–LSPUM method (3.30). *Right: SSP2(3,3,2)–LPUM method* (4.2).

Results III

Method	$\Delta t_{\max}$	Δt_{mean}	$\text{CFL}_{\max}$	CFL_{mean}	$\text{CFL}_{\text{start}}$	Time
SSP2(2,2,2)–PM, γ=0.24 (53)	26.02 s	15.02 s	1.22	0.7	0.5	01:55:47
SSP2(3,3,2)–LUM (54)	79.60 s	48.33 s	3.7	2.24	0.4	00:51:58
SSP2(3,3,2)–LSPUM (15)	125.14 s	75.53 s	5.8	3.5	0.3	00:45:17
SSP2(3,3,2)–LPUM (18)	179.54 s	86.79 s	8.31	4.02	0.3	00:31:16
SSP2(3,3,2)–LPM (21)	58.57 s	38.51 s	2.71	1.8	0.3	00:57:23
SSP1(1,1,1)–LPM (52)	15.33 s	1.15 s	0.71	0.053	0.05	9:36:12

Table 2: Simulation of double-diffusive convection: Time–steps, CFL–numbers and wallclock-times over the first 80 scrt.

again a case with Pr = Le = 0.05, 429 × 428 points,
VSC-1 @ 64 CPUs but this time based on parallel multigrid solver (see Higueras et al. (2013), to be submitted)

...THANK YOU FOR YOUR TIME !